Theory for Hinged Wavemakers of Finite Draft in Water of Constant Depth

Jae Min Hyun*
Korea Institute of Science and Technology, Seoul, Korea

Extending the theoretical work of Biesel, a study is made of a flap-type wavemaker hinged in the middle of a wall. The first-order linearized hydrodynamic equations of motion are solved to obtain the velocity potential, which is composed of a wave part and a spatially transitory part. Characteristics of generated waves far away from the wavemaker are analyzed as to the wave profile, flap stroke, water particle excursions, and power consumption of the wavemaker. The importance of the spatially transitory part is discussed with regard to the role played by the inertia pressure, which gives rise to added inertia of the flap. Surface elevations very near the flap are found. The hydrodynamically induced torque and the total hydrodynamic force on the flap are computed. The computed results seem to be well explained by the differing behaviors of the normal pressure and of the inertia pressure with increasing water depth.

Introduction

THE theoretical foundation of laboratory wave-generating apparatus was developed in detail by Biesel[1] and coworkers of Grenoble, pertaining to two-dimensional irrotational motions in prismatic channels of rectangular cross-section. Following the classical wavemaker theory of Havelock, Biesel solved the first-order linearized hydrodynamic equations of motion to find the resultant wave motions caused by a wavemaker at one end of a channel. As examples, he considered two simple cases, namely, a piston-type wavemaker, and a flap-type wavemaker hinged at the bottom of a wall. A brief comparison was made of the two types of wavemaker with regard to the quality of generated waves, wavemaker stroke, and the total hydrodynamic force applied at the wavemaker. The validity of the first-order wavemaker theory was experimentally verified by Ursell, Dean, and Yu,[2] with particular reference to a piston-type wavemaker.

For all practical purposes, however, flap-type wavemakers in common use today are fabricated with their lower ends hinged in the middle of the wall, unlike the simple flap-type wavemaker investigated by Biesel. An article by Taniguchi and Shibata[3] reported that agreement was satisfactory between the predictions of the first-order wavemaker theory and the measurements conducted in the Mitsubishi Nagasaki experimental tank. The Nagasaki tank was equipped with a flap-type wavemaker, whose flap draft (the distance from the undisturbed mean water surface to the lower hinges of the flap) was 1.77 m, and the constant water depth was 6.31 m. Their measurements dealt with flap frequency, flap stroke, wave profile, and the reaction force at the piston rod of the hydraulic drive.

As was pointed out by Taniguchi and Shibata, published theses on wavemakers are rather scarce, and few scattered technical data for wavemaker performance are available in the literature. In most descriptive reports of existing towing tank facilities,[4,5,6] wavemakers seem to be somewhat cursorily treated without providing much technical information.

A unified account of a flap-type wavemaker, including detailed analysis of the added inertia effect of the flap, which was not previously discussed, is presented here. Relevant theoretical considerations, based on the first-order linearized hydrodynamic equations of motion, are given and possible analytical approaches are used. Treating the flap draft as a parameter, numerical computations are carried out to study the quality of generated waves and the hydrodynamically induced force and torque on the flap. The added inertia effect of the flap, which is a consequence of the spatially transitory part of fluid motion, is closely examined with respect to the flap torque augmentation and water particle displacements near the wavemaker. The analysis of a flap-type wavemaker is of practical usefulness in that it can be utilized for more general purposes, including the determination of the added mass and the damping coefficient of thin vertical bodies in water.

Received May 19, 1975; revision received July 29, 1975.
Index categories: Hydrodynamics; Wave Motion and Sloshing; Research Facilities and Instrumentation.
*Investigator, Shipbuilding Industry Technical Services.

General Formulation

Let us consider two-dimensional irrotational motions of an inviscid, incompressible fluid in a semi-infinite channel ($0 \leq x < \infty$) with rectangular cross section of width B and of constant water depth h. The coordinate system and the schematic diagram of the wavemaker arrangement are shown in Fig. 1.

The velocity potential $\phi(x, y, t)$ for small-amplitude waves generated by a simple-harmonic flap motion about $x=0$ is governed by the Laplace equation

$$(\partial^2\phi/\partial x^2) + \partial^2\phi/\partial y^2 = 0 \quad 0 \leq x < \infty \quad 0 \leq y \leq h \tag{1}$$

with the associated boundary conditions

$$\partial\phi/\partial y = 0 \quad \text{on} \quad y = 0 \tag{2}$$

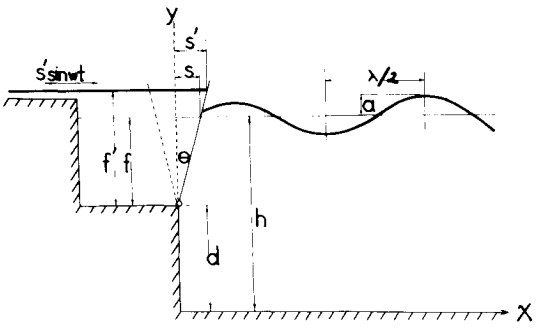

Fig. 1 Schematic diagram of flap-type wavemaker.

$$\omega^2\phi+g(\partial\phi/\partial y)=0 \quad \text{on} \quad y=h \tag{3}$$

$$(\partial\phi/\partial x)=\omega\xi(y)\cos\omega t \quad \text{on} \quad x=0 \tag{4}$$

and, at large values of x, the solution is chosen to represent waves propagating towards $x=\infty$, thus radiation condition at $x=\infty$ is imposed. Here ω is the angular frequency of the flap motion, g is the gravitational acceleration. $\xi(y)$ denotes the prescribed maximum displacement of the flap surface such that

$$x=\xi(y)\ \sin\omega t \tag{5}$$

at each instant describes the location of the contact surface between the flap and water. The correctness of the contact surface boundary condition Eq. (4) is discussed in depth by Biesel, and we shall use Eq. (4) here, assuming that the maximum flap angle is small so that the particle displacements from the mean flap position $x=0$ are also small.

The velocity potential ϕ is known to be[1,2]

$$\phi=-\frac{\omega}{k}A\cosh(ky)\sin(\omega t-kx) - \sum_{n=1}^{\infty}\frac{\omega}{k_n}A_n\cos(k_ny)\exp(-k_nx)\cos\omega t \tag{6}$$

in which k, the wavenumber of a generated wave of wavelength $\lambda(\equiv 2\pi/k)$, is the positive real root of the dispersion relation $\omega^2=gk\tanh(kh)$, while k_n's are the positive real roots of $\omega^2=-gk_n\tan(k_nh)$. The coefficients A, A_n's are to be determined from Eq. (4), such that

$$A\cosh(ky)+\sum_{n=1}^{\infty}A_n\cos(k_ny)=\xi(y) \tag{7}$$

whence we have

$$A=\frac{2k\int_0^h\xi(y)\cosh(ky)\,dy}{\sinh(kh)\cosh(kh)+kh} \tag{8}$$

$$A_n=\frac{2k_n\int_0^h\xi(y)\cos(k_ny)\,dy}{\sin(k_nh)\cos(k_nh)+k_nh} \tag{9}$$

Having obtained the complete set of coefficients defining the velocity potential, we can proceed to describe the orbital motion of an individual water particle whose mean position is given by the initial coordinate x and y. The displacements of a water particle in the x and y directions are[1]

$$X=A\cosh(ky)\sin(\omega t-kx) + \sum_{n=1}^{\infty}A_n\cos(k_ny)\exp(-k_nx)\sin\omega t \tag{10}$$

$$Y=A\sinh(ky)\cos(\omega t-kx) + \sum_{n=1}^{\infty}A_n\sin(k_ny)\exp(-k_nx)\sin\omega t \tag{11}$$

respectively.

It is evident that the fluid motion is composed of two parts: a wave part propagating in the positive x direction, and a sum of terms of which each decays exponentially as $\exp(-k_nx)$. Obviously, provided that no dissipation is considered in the analysis, the wave part of the fluid motion persists in the entire length of the channel, whereas the exponentially decaying part, which is spatially "transitory" in nature, is present only in the vicinity of the wavemaker. It can be readily shown that $(n-\frac{1}{2})\pi<k_nh<n\pi$, thus, even the most slowly decaying term, which is associated with k_1, is reduced to 0.01 of its original value after traveling a distance of $3h$. Therefore, the influence of these spatially transitory terms virtually disappears when $x>3h$, but their role is crucial in the determination of the forces exerted on the wavemaker and to wave profile distortions near the wavemaker. In fact, the total hydrodynamic force acting on the flap is, under certain conditions, attributable to the dominant influence of these spatially transitory terms.

In connection with Eq. (11), the wave amplitude a at a large distance away from the wavemaker (say $x>3h$) is[1]

$$a=A\sinh(kh) \tag{12}$$

With the aid of Bernoulli's theorem, the pressure p is obtainable from Eq. (6)

$$p=-\rho(\partial\phi/\partial t)+\rho g(h-y)-\rho q^2/2 =p_w+p_i+\rho g(h-y)-\rho q^2/2 \tag{13}$$

where ρ is the water density, $\rho g(h-y)$ is the hydrostatic pressure, q is the velocity of water particle, and

$$p_w=\rho ga[\cosh(ky)/\cosh(kh)]\cos(\omega t-kx) \tag{13a}$$

$$p_i=\sum_{n=1}^{\infty}\rho gA_n\tan(k_nh)\cos(k_ny)\exp(-k_nx)\sin\omega t \tag{13b}$$

Clearly, p_w, often called the normal pressure, represents the wave part of the hydrodynamic pressure fluctuations, and p_i, designated as the inertia pressure by Biesel, is seen to come from the spatially transitory part of ϕ. The normal pressure p_w at the wavemaker $x=0$ is in phase with the flap velocity, which must, therefore, require that a finite amount of work be done over one cycle. This energy expenditure is consumed in the form of propagation of outgoing waves on the free surface. On the other hand, the inertia pressure p_i, which is in phase with the acceleration of the flap, does no work on the average; however, the major part played by p_i turns up in the form of added inertia of the flap. In the jargon of naval hydrodynamics, p_w and p_i are associated with the damping coefficient and added mass, respectively.

In summary, the problem narrows down to the calculation of ω, k_n's, A, A_n's, if the constant water depth h, the desired wavelength λ, and the contact surface equation $\xi(y)$ are provided.

Specialization to Flap-type Wavemaker

Let us now specialize the general formulation to a flap-type wavemaker. The flap draft is designated as f, and the maximum flap stroke at the mean water level is denoted by S. To satisfy the aforementioned contact surface boundary condition Eq. (4), it is assumed that the maximum flap angle $\theta=\arctan(S/f)$ is small. Accordingly, the contact surface equation $\xi(y)$ is given as

$$\xi(y)=(S/f)(y-d) \quad \text{for} \quad d\le y\le h$$
$$\xi(y)=0 \quad \text{for} \quad y<d \tag{14}$$

where $d=h-f$.

Upon substitution of Eq. (14) into Eqs. (8) and (9), A and A_n's are found, containing f as a parameter

$$A=2S\,\frac{kf\sinh(kh)-\cosh(kh)+\cosh(kd)}{kf[\sinh(kh)\cosh(kh)+kh]} \tag{15}$$

$$A_n=2S\,\frac{k_nf\sin(k_nh)+\cos(k_nh)-\cos(k_nd)}{k_nf[\sin(k_nh)\cos(k_nh)+k_nh]} \tag{16}$$

Subsequently, the wave amplitude a is obtained from Eqs. (12) and (15)

$$a=2S\frac{[kf\sinh(kh)-\cosh(kh)+\cosh(kd)]\sinh(kh)}{kf[\sinh(kh)\cosh(kh)+kh]} \tag{17}$$

The ratio of the wave amplitude to the flap stroke at the mean water level a/s takes a limiting value of 2 in the case of very short waves ($kh>>1$), regardless of the flap draft. However, in the case of waves of finite length, a/s shows a marked dependence on f as well as on λ/h.

The power necessary to drive the flap P excluding any mechanical and frictional losses, to generate a sinusoidal wavetrain of wavelength λ can be computed as

$$P=2B\int_d^h (p_w+p_i)_{x=0}\omega\xi(y)\cos\omega t\,dy$$

$$=P_1(\cos\omega t)^2+P_2\cos\omega t\sin\omega t \tag{18a}$$

where

$$P_1=2B\rho gahS\omega\left\{\frac{1}{\cosh(kh)}\left[\frac{\sinh(kh)}{kh}-\frac{1}{(kh)^2}\left[\frac{h}{f}\right](\cosh kh-\cosh kd)\right]\right\} \tag{18b}$$

$$P_2=2B\rho gS\omega\left\{\sum_{n=1}^{\infty}A_n\tan(k_nh)\left[\frac{1}{k_n^2f}(\cos k_nh-\cos k_nd)+\frac{\sin k_nh}{k_n}\right]\right\} \tag{18c}$$

In Eq. (18a), the factor of 2 takes into account that water fills in both sides of the flap. In the case of the flap-type wavemaker with water in both sides of the flap, the hydrostatic pressure $\rho g(h-y)$ balances on either side of the flap. By the same token, the velocity pressure head $-\rho q^2/2$ in Eq. (13a), which is usually neglected in linearized equations anyway, makes no contribution to force or torque calculations. It should be noted that, in the case of the flap-type wavemaker without water on the back side, as investigated by Taniguchi and Kasai,[7] the contribution from the hydrostatic pressure normally outweighs that from the hydrodynamic pressure in force and torque calculations. In the wavemaker under consideration, it is assumed that a suitably designed wave absorber is in operation behind the flap ($x<0$).

If we take the mean value of P over one cycle, the second term of Eq. (18a), which comes from p_i, makes no contribution, and only the first term, which is associated with p_w, remains. Thus, the mean power over one cycle $\bar{P}$ may be expressed as

$$\bar{P}=P_1/2 \tag{19}$$

The torque exerted on the flap about the lower hinge by the hydrodynamic pressure, taking into account both sides of the flap, may be computed as

$$T=2B\int_d^h (p_w+p_i)_{x=0}(y-d)\,dy=T_c\cos\omega t+T_s\sin\omega t \tag{20a}$$

where

$$T_c=2B\rho gah^2\left\{\frac{1}{\cosh kh}\right\}\left\{\frac{f\sinh kh}{kh^2}-\frac{1}{(kh)^2}(\cosh kh-\cosh kd)\right\} \tag{20b}$$

$$T_s=2B\rho gh^2\sum_{n=1}^{\infty}A_n\tan(k_nh)\left[\frac{\cos k_nh-\cos k_nd}{(k_nh)^2}+\frac{f\sin k_nh}{k_nh^2}\right] \tag{20c}$$

Evidently, T_c arises from the normal pressure p_w, whereas T_s is related to the inertia pressure p_i.

By integrating the hydrodynamic pressure itself, we may calculate the total hydrodynamic force acting on the flap

$$F=2B\int_d^h (p_w+p_i)_{x=0}dy=F_c\cos\omega t+F_s\sin\omega t \tag{21a}$$

$$F_c=2B\rho gah\left\{\frac{\sinh kh-\sinh kd}{kh\cosh kh}\right\} \tag{21b}$$

$$F_s=2B\rho gh\left\{\sum_{n=1}^{\infty}\frac{A_n\tan(k_nh)[\sin k_nh-\sin k_nd)}{k_nh}\right\} \tag{21c}$$

In actual design work, we like to know the total torque T_t that the wavemaker flap has to compensate. The total torque is the sum of the hydrodynamically induced T of Eq. (20a) and the pure inertia moment T_i of the flap itself. The pure inertia moment T_i can be expressed as

$$T_i=(f'S'/3g)\bar{W}\omega^2\sin\omega t \tag{22}$$

where $\bar{W}$ is the net weight of the flap.

The force applied at the piston rod of the hydraulic drive system F_p may then be calculated as

$$F_p=T_t/f' \tag{23}$$

whence the reaction force that the lower hinges of the flap have to support can be found by the difference between F_p and F.

Numerical Computations

In the wavelength range of practical interest $0.2\le\lambda/h\le5.0$, numerical computations are performed to examine the quality of generated waves and the hydrodynamic effects on the wavemaker. Figure 2 displays a/s, the ratio of the wave amplitude to the flap stroke, as a function of flap draft and of wavelength. As was pointed out previously, in the case of very short waves a/s reaches the limiting value of 2 regardless of f/h; however, a noted dependence of a/s on f/h is seen for finite wavelengths.

The mean power consumption of the flap, $\bar{P}$, as shown in Fig. 3, is a function of wave profile alone. Obviously, $\bar{P}$ is independent of the particular geometrical shape of the flap, since P is the energy input that is recovered in the output in the form of propagation of waves. This argument is, of course, based on inviscid, nondissipative fluid motion, disregarding any mechanical and frictional energy losses incurred in actual wave-generating apparatus.

The finite depth effect may be detected in a number of ways. Figure 4 shows the normal pressure P_w as a function of varying water depth. For short waves (say $\lambda/h<1.0$), p_w is pronounced only near the water surface, enabling the problem to be treated essentially as deep-water waves. With increasing wavelengths p_w is felt into increasing water depths, making the finite depth effect nonnegligible. Another way to see the finite depth effect is to compute the particle excursions far away from the wavemaker, as shown in Figs. 4 and 5. (The plot of the particle excursions in the x direction becomes the same as Fig. 4, if the abscissa of Fig. 4 is replaced by X/a). In the case of short waves, particle excursions in the x and y directions are almost identical, so that particle orbits are

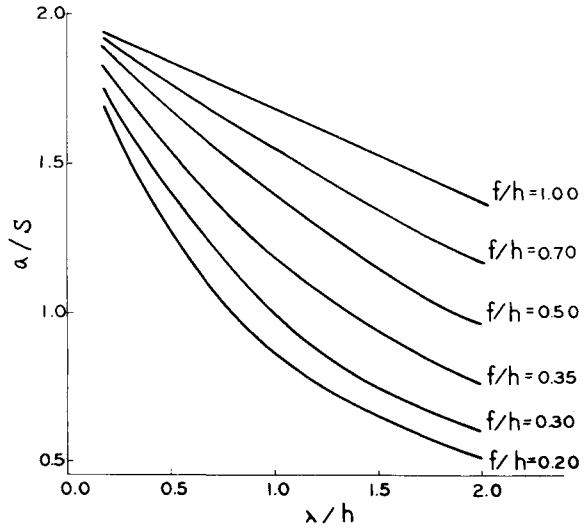

Fig. 2 Wave amplitude as function of wavelength and flap draft.

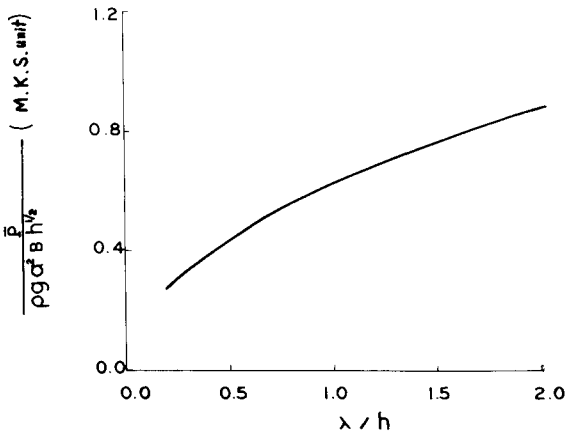

Fig. 3 Mean power comsumption of flap-type wavemaker.

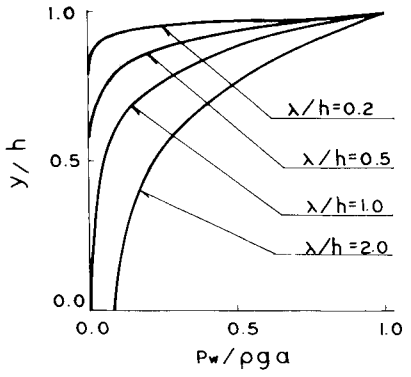

Fig. 4 Normal pressure as function of water depth.

nearly circular. This is a well-known aspect of deep-water wave motions. The finite depth effect is manifested for long waves, where individual particle orbits are ellipses rather than circles, with the maximum x and y excursions as major and minor axes, respectively.

Turning now to the question of spatially transitory part, a sum of terms of which each decays exponentially as $\exp(-k_n x)$. As was discussed previously, these spatially transitory terms do not affect the dynamic characteristics of waves far away from the wavemaker (say $x>3h$); however, they play a central role in determining fluid motions near the wavemaker. For a given λ/h, an infinite number of k_n's are available, but the first few terms are of dominant importantance. In actual numerical computations, we terminated the series up to the first 10 terms to insure an accuracy of less than 1%.

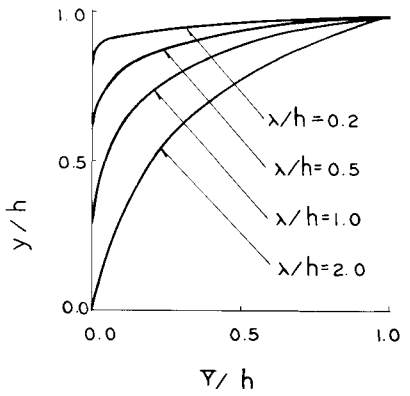

Fig. 5 Water particle excursion in y direction far away from the wavemaker.

The inertia pressure p_i, the sin ωt part of the hydrodynamic pressure expressed in Eq. (13a), is plotted in Fig. 6. A ready comparison can be made between p_w and p_i; throughout the water depth on the whole p_i sustains its presence substantially, contrary to p_w, which invariably decreases rapidly with increasing depth. In particular, in the case of short waves, for instance $\lambda/h=0.2$, Fig. 6d demonstrates the overwhelming influence of p_i over p_w except in a narrow region proximate to the water surface. With increasing wavelengths, the relative magnitude of p_i over p_w is diminishing gradually, but the effect of p_i remains noticeable. By observing the variation of p_i with respect to the flap draft, we may conclude that shorter flap drafts are more attractive for generating short waves from the standpoint of reducing the magnitude of p_i. Large magnitudes of p_i are undesirable in that p_i essentially augments the inertia of the flap, resulting in increased torque to be compensated by the flap drive. At the same time, a large magnitude of p_i near the tank bottom causes leakage through the flap base, which gives rise to energy losses and wave profile distortions. Thus, when it is desired to generate short waves, Figs. 6c and 6d illustrate that p_i could be significantly reduced by shortening the flap drafts accordingly.

Turning to the effect of the spatially decaying terms of the water particle displacements, we first evaluate Eq. (11) at $x=0$, $y=h$ to obtain the surface elevation in the vicinity of the flap. For the sake of definiteness, we set $\omega t=\pi/2$, which corresponds to the most advanced position of the flap. At this particular instant, the surface elevation very close to the flap is entirely represented by the second term of Eq. (11), with the contribution from the wave part being zero. Therefore, this particular surface elevation denotes the maximum wave amplitude distortion occurring very near the flap. Table 1 shows this maximum wave amplitude distortion for varying wavelengths and flap drafts. It is noteworthy that, for a given flap draft, the smallest wave amplitude distortion appears to be located roughly along the diagonal line of Table 1, from the upper left corner to the lower right corner.

The total particle displacement in the x direction very near the flap when the flap is at its most advanced position ($\omega t=\pi$

Table 1 Water surface elevation at $x=0$, $\omega t=\pi/2$, nondimensionalized by wave amplitude a

$f/h=1.00$		$f/h=0.50$	$f/h=0.35$	$f/h=0.25$	$f/h=0.15$
$\lambda/h=5.0$	−0.1358	−0.4224	−0.5659	−0.6940	−0.8270
$\lambda/h=2.0$	0.1478	−0.1330	−0.2658	−0.3845	−0.5035
$\lambda/h=1.0$	0.4033	0.1304	−0.0055	−0.1308	−0.2555
$\lambda/h=0.5$	0.5970	0.3371	0.2009	0.0665	−0.0714
$\lambda/h=0.3$	0.6871	0.4365	0.3058	0.1665	0.0202

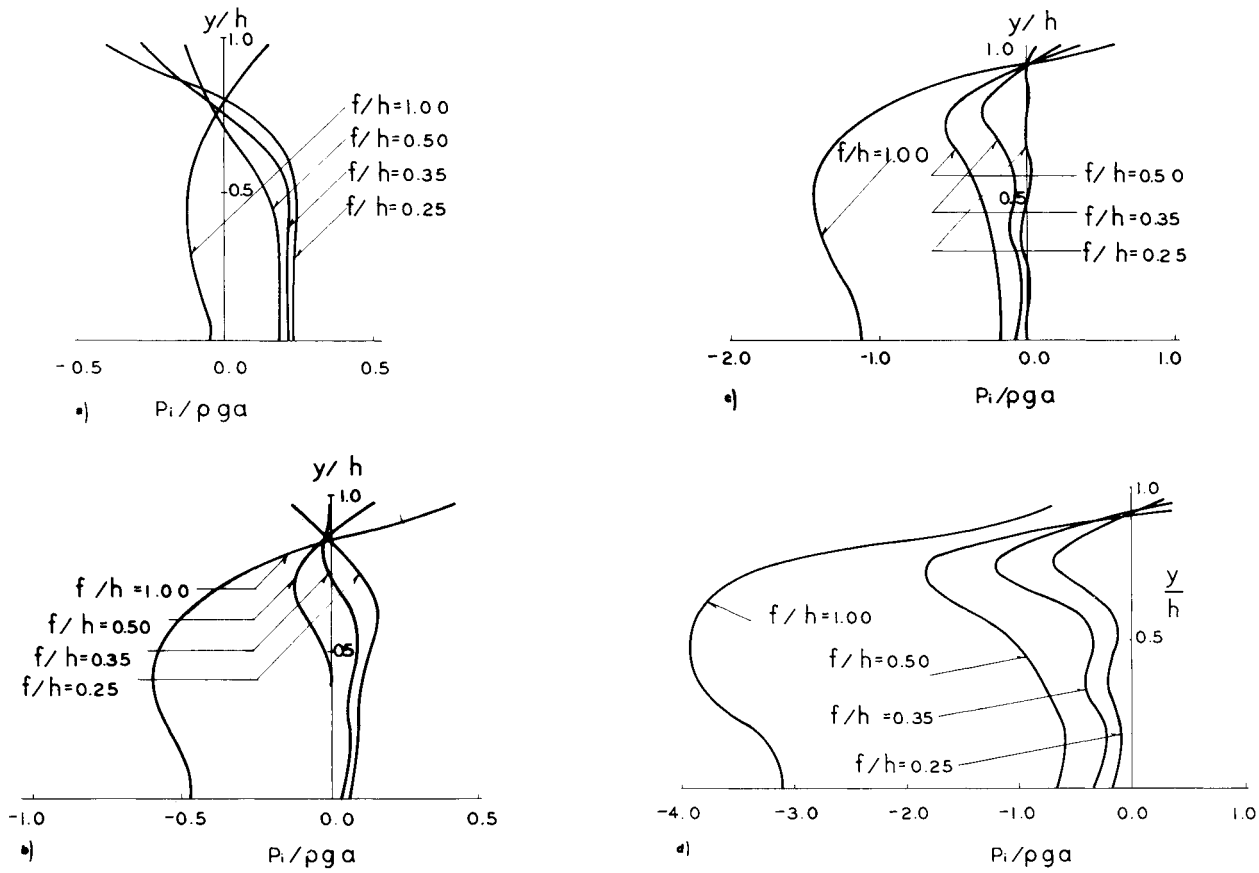

Fig. 6 Inertia pressure as function of water depth, for case of a) $\lambda/h=2.0$, b) $\lambda/h=1.0$, c) $\lambda/h=0.5$, d) $\lambda/h=0.2$.

/2) is contributed by both the wave part and the spatially transitory part of Eq. (10). Figure 7 displays the deviation of the particle displacement from the actual flap position. The deviation is appreciable when generating a short wave by use of a short flap draft. In this situation, the flap angle has to increase accordingly, therefore, the basic assumption of small flap angle is poorly satisfied. It is suggested that an improvement in the first-order formulation is called for to account for this appreciable deviation of the particle displacement from the flap location.

The hydrodynamically induced torque T and the total hydrodynamic force acting on the flap F, expressed in Eqs. (20a) and (21a) are shown in Table 2 in the form of $M\cos(\omega t-\alpha)$. The minimum values of M seem to be located approximately along the diagonal line in Table 2, stretching from the upper left corner to the lower right corner. This can be explained in conjunction with the differing behaviors of p_w and p_i. The normal pressure p_w reaches ρga on the water surface, and it decreases rapidly with water depth. The rate of decrease of p_w is largely dependent on λ/h, as shown in Fig. 4. On the other hand, p_i has a strong dependence on both λ/h and f/h, as can be seen in Fig. 6.

With $f/h=1.00$, the miminum values of T and F are attained when the generated waves are moderately long (say $\lambda/h\cong 2.00$). If a flap-type wavemaker with $f/h=1.00$ is used to generate short waves (say $\lambda/h=0.20$), p_i overwhelms p_w (the phase angle α becomes close to $-\pi/2$), resulting in large torque and hydrodynamic force on the flap. In the case of a small flap draft, e.g., $f/h=0.15$, we find the minimum values of T and F when generated waves are quite short. Since the flap is immersed only in the region a short distance away from the water surface, p_w is still largely unattenuated in the region of flap immersion, even for short waves. On the other hand, the influence of p_i is weak when generating short waves by use of short flap drafts, as illustrated in Figs. 6c and 6d. Consequently, if small flap drafts are in use, the primary contributions to T and F come from p_w (the phase angle α is close to zero). From the standpoint of a wavemaker designer, we

Table 2 Hydrodynamically induced torque T and total hydrodynamic force on the flap F, nondimensionalized by $2B\rho gah^2$, $2B\rho gah$, respectively. Both quantities are expressed in form of $M\cos(\omega t-\alpha)$

		$f/h=1.00$		$f/h=0.50$		$f/h=0.35$		$f/h=0.25$		$f/h=0.15$	
		M	α	M	α	M	α	M	α	M	α
$\lambda/h=2.0$	T	0.2248	−0.0534	0.0795	−0.0914	0.0447	−0.1865	0.0255	−0.2847	0.0106	−0.4146
	F	0.3214	−0.1627	0.2540	−0.0169	0.2142	−0.1015	0.1771	−0.2004	0.1279	−0.3600
$\lambda/h=1.0$	T	0.1904	−0.7911	0.0554	−0.0591	0.0332	−0.0241	0.0197	−0.0724	0.0086	−0.1946
	F	0.4177	−1.1799	0.1545	−0.1684	0.1415	−0.0060	0.1261	−0.0039	0.0980	−0.1320
$\lambda/h=0.5$	T	0.4606	−1.4111	0.0454	−0.7425	0.0223	−0.2486	0.0138	−0.0301	0.0066	−0.0339
	F	1.0929	−1.4979	0.1856	−1.1286	0.0957	−0.6073	0.0768	−0.1316	0.0675	0.0141
$\lambda/h=0.3$	T	0.8901	−1.5197	0.0810	−1.3009	0.0241	−0.9279	0.0103	−0.3510	0.0050	−0.0060
	F	2.0152	−1.5471	0.3747	−1.4430	0.1585	−1.2651	0.0694	−0.8165	0.0457	−0.0426
$\lambda/h=0.2$	T	1.4186	−1.5492	0.1395	−1.4638	0.0397	−1.3126	0.0113	−0.9063	0.0038	−0.1103
	F	3.1599	−1.5607	0.6244	−1.5198	0.2753	−1.4549	0.0115	−1.2814	0.0338	−0.3682

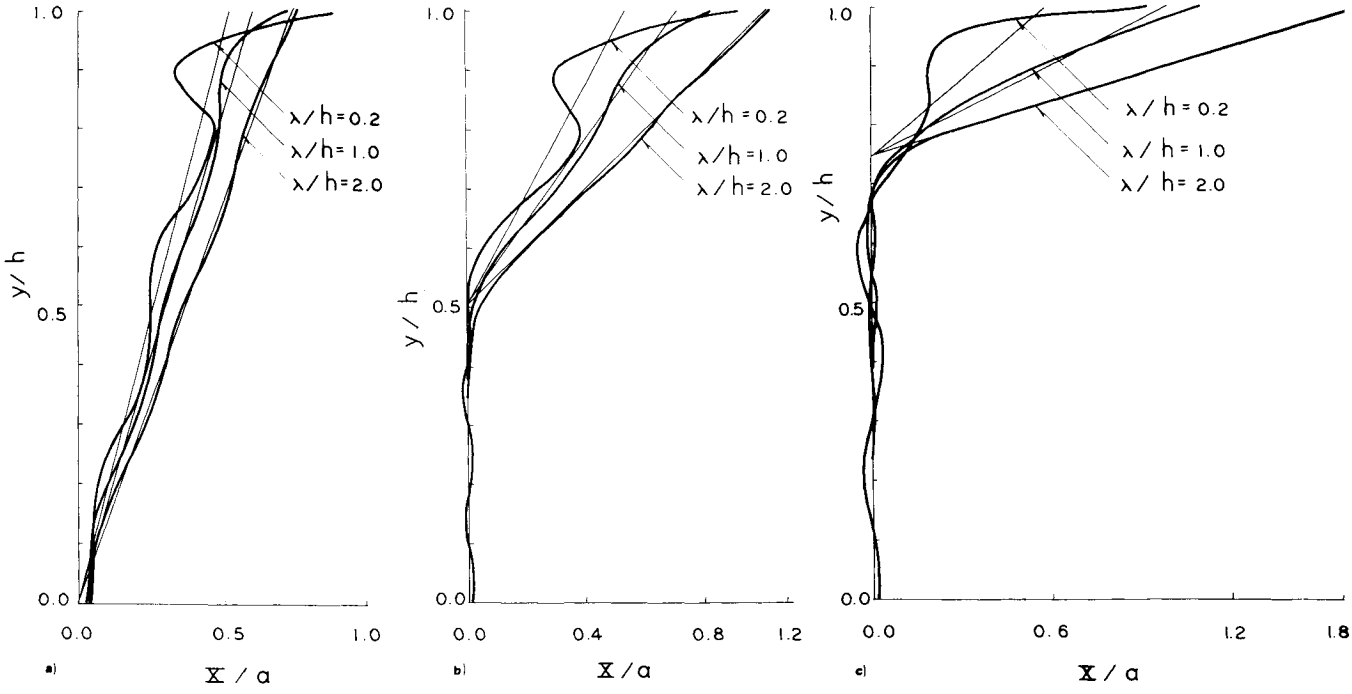

Fig. 7 Water particle displacement in x direction very near flap, for case of a) $f/h = 1.00$, b) $f/h = 0.50$, c) $f/h = 0.25$. Straight lines denote most advanced flap positions.

would like to choose a flap size which will need less torque and hydrodynamic force on the flap. The diagonal line of Table 2 may suggest a recommended range of flap draft in this regard. We recall a similar conclusion was reached in Table 1 with a view towards reducing the wave profile distortion near the wavemaker.

Conclusion

A unified account has been given of a flap-type wavemaker, treating the flap size as a parameter. Major points of practical usefulness to a flap-type wavemaker design are obtained, i.e., the quality of generated waves, power requirement, and the hydrodynamically induced torque and force on the flap. Differing behaviors of the normal pressure and the inertia pressure determine the dynamic characteristics of fluid motions caused by the wavemaker. The added mass effect of the flap is discussed in some detail in connection with the role played by the inertia pressure. A recommended range of flap size is presented with a view towards reducing both the wave profile distortion near the wavemaker and the hydrodynamic load on the flap. The results of the present analysis on flap-type wavemakers should be the subject of further experimental study.

References

[1] Biesel, F., "Etude theorique d'un certain type d'appareil a houle," *La Houille Blanche,* No. 2, 1951. English Translation in Project Rept. 39, March 1954, St. Falls Hydraulic Lab., Univ. of Minnesota, Minneapolis, Minn.

[2] Ursell, F., Dean, R.G., and Yu, Y.S., "Forced Small-Amplitude Water Waves: A Comparison of Theory and Experiment," *Journal of Fluid Mechanics,* Vol. 7, Part 1 1959, pp. 33-52.

[3] Taniguchi, K. and Shibata, J., "Wavemaker of Mitsubishi Nagasaki Experimental Tank," Yugoslav Ship Hydrodynamics Inst., No. 9, Sept. 1960, pp. (17-1)-(17-23).

[4] Vosper, A.J., Facilities and Ship-Model Instrumentation at the Admiralty Experiment Works Haslar," Yugoslav Ship Hydrodynamics Inst. No. 9, Sept. 1960, pp. (3-1)-(3-37).

[5] Orchard, D.R., Woolfson, M., and Shearer, J.R., "The Design, Construction and Operation of No. 3 Towing Tank," Symposium on Experiment Facilities for Ship Research in Great Britian, Ship Div., National Physical Lab., Teddington, England, May 1967.

[6] "On the Mitaka No. 2 Ship Model Experiment Tank of Ship Research Institute," Ship Propulsion Div., Ship Research Inst. Rept., Vol. 6, No. 4, 1969, SRI, Ministry of Transport, Japan.

[7] Taniguchi, K. and Kasai, H., "A New-Type Flap-Type Wavemaker Without Water on Back Side," *Fall Meeting of Society of Naval Architects of Japan,* 1972, pp. 129-136.